Implementation of a model taking into account the asymmetry between tension and compression, the temperature effects in a finite element code for shape memory alloys structures calculations

Frédéric Thiebaud, Christian Lexcellent, Manuel Collet, Emmanuel Foltete

Implementation of a model taking into account the asymmetry between tension and compression, the temperature effects in a finite element code for shape memory alloys structures calculations

Frederic Thiebaud *, Christian Lexcellent, Manuel Collet, Emmanuel Foltete

Institut Femto-ST, Department LMARC, 24 rue de l'epitaphe, 25000 Besancon, France

Shape memory alloys (SMAs) are good candidates for being used as passive dampers, strain sensors, stiffness or shape drivers. To design these structures, an implementation which takes into account the obvious asymmetry between tension–compression and the thermomechanical coupling taken into account with the introduction of the heat equation is required. We present in this paper an implementation of a phenomenological model based on the R_L model (Raniecki and Lexcellent [B. Raniecki, C. Lexcellent, Eur. J. Mech. A/Solids 17 (2) (1998) 185–205]) in a finite element code called COMSOL© which allows to build automatically many loading cases in force or displacement. The results clearly show the influence of the temperature on the pseudoelastic behavior of SMA and on the asymmetry between tension and compression. This implementation could be useful to simulate complex three dimensional SMA structures as dynamical devices.

Keywords: Shape memory alloys; Asymmetry tension–compression; Heat equation; Multiphysic coupling

1. Introduction

In problems involving SMA materials, thermomechanical coupling has to be taken into account due mainly to the latent heat associated to the martensitic transformation and heat production/absorption resulting from SMA material by internal dissipation process. Raniecki and Lexcellent [1] have developed a thermodynamic three dimensional model of SMA behavior taking into account:

- relevant kinetic laws of thermoelastic martensitic transformation,
- asymmetry of stress–strain curves under tension and compression, symmetry in pure shear.

The experience shows that taking into account both heat equation and the asymmetry of stress–strain curves is not obvious to implement into a finite element code. Although this asymmetry and the heat equation coupling are important parameters of the pseudoelastic behavior of SMA, most of numerical implementation are leaded without its.

Thus, the aim of this paper is to present a clear implementation of the so called R_L model [1]. At first a phenomenological model at the macroscopic scale in the frame of the thermodynamics of irreversible process devoted to multiaxial pseudoelasticity [1] is recalled. In a second part, this model is implemented in a finite element code. The software COMSOL© have been chosen because of its facilities to solve multiphysic coupled problems which is the case for phase transition linked to the heat equation. In order to validate the implementation, some tests are performed: a plate in tension and a plate under bending in its plane, for three different thermal simulations: isothermal, adiabatic and with an external imposed temperature on the

* Corresponding author. Tel.: +33 381666008; fax: +33 381666700.
E-mail addresses: frederic.thiebaud2@univ-fcomte.fr, fred.thiebaud@libertysurf.fr (F. Thiebaud).

edge. Finally, rate effects are shown by loading a plate in tension with different force rates.

2. A thermomechanical model for the pseudoelasticity

2.1. Thermodynamical potential functions

Modeling material behavior needs classically a choice of a thermodynamic potential and also a dissipation potential function or alternatively some yield functions of phase transformation initiation (as it is the scheme in plasticity). Hence, a Helmholtz free energy and two yield functions, the first for the forward phase transformation ($A \rightarrow M$) and the second for the reverse phase transformation ($M \rightarrow A$) are chosen. The model initiated by Raniecki et al. [2] has been written in order to fit multiaxial loading.

Let consider a representative volume element (RVE) of SMA in a single solid phase state at the reference stress state $\underline{\sigma} = \underline{0}$ and at the reference temperature $T = T_0$ ($T_0 > A_f^0$). This phase is called austenite A. Its properties will be denoted by index $\alpha = 1$. Under applied thermomechanical loading, austenite can be transformed into martensite M. The properties of martensite will be denoted by index $\alpha = 2$.

Some studies performed by [3,4] have shown the martensite partition: the austenite can be transformed in a self-accommodating martensite M_t by pure cooling or in stress induced martensite M_σ under pure mechanical loading. In our study, this partition is not taken into account because of the loading which is only mechanical.

Suppose that a non-equilibrium state of two phases RVE is described by the following variables:

- $\underline{\varepsilon}_\alpha$: the strain tensor of each phase ($\alpha = 1, 2$),
- T: the actual temperature,
- ξ: the fraction of martensite,
- h_k ($k = 1, \ldots, n$): a set of internal variables.

Generally, h_k are variables of displacement type. They represent the RVE internal pattern rearrangements at the micro-scale level.

The following form of the specific free energy ϕ_n of a two phases mixture is chosen as

$$\phi_n(T, \underline{\varepsilon}_\alpha, \xi, h) = (1-\xi)\phi_1 + \xi\phi_2 + \Delta\phi \tag{1}$$

where

$$\Delta\phi = \xi(1-\xi)\phi_{it}(T) \tag{2}$$

$$\phi_{it} = \bar{u}_0 - T\bar{s}_0. \tag{3}$$

ϕ_{it} represents some configurational energy associated with the coherency of phases. For most cases: $\bar{s}_0 = 0$, thus ϕ_{it} is constant ($\phi_{it}(T) = \phi_{it}$). The exact form of $\Delta\phi$ remains an open problem since it strongly depends on the incompatibilities between the martensite platelets and between martensite and austenite. Sometimes, $\bar{u}_0(\bar{s}_0)$ is called internal configurational energy (entropy). Both phases are regarded as thermoelastic solids such that

$$\phi_\alpha(T, \underline{\varepsilon}_\alpha, \xi, h) = u_0^\alpha - Ts_0^\alpha + \frac{1}{2\rho}[\underline{\varepsilon}_\alpha - \underline{\varepsilon}_\alpha^{\mathrm{tr}} - \underline{\varepsilon}_\alpha^{\mathrm{th}}] : \underline{\underline{L}}[\underline{\varepsilon}_\alpha - \underline{\varepsilon}_\alpha^{\mathrm{tr}} - \underline{\varepsilon}_\alpha^{\mathrm{th}}] + C_v\left[(T-T_0) - T\ln\frac{T}{T_0}\right]$$

where ρ is the mass density, T_0 is the reference temperature, u_0^α is the internal energy of the α phase and s_0^α is the internal entropy of the α phase.

The elastic stiffness tensor $\underline{\underline{L}}$, the thermal expansion coefficient α and the specific heat C_v are supposed independent of the phase state. The thermal strain tensor and the elastic strain tensor are respectively:

$$\underline{\varepsilon}_\alpha^{\mathrm{th}} = \underline{\varepsilon}^{\mathrm{th}} = \alpha(T-T_0)\mathbb{I} \tag{4}$$

$$\underline{\varepsilon}_\alpha^{\mathrm{el}} = \underline{\varepsilon}^{\mathrm{el}} = \underline{\underline{L}}^{-1}\underline{\sigma} = \underline{\varepsilon} - \underline{\varepsilon}^{\mathrm{tr}} - \underline{\varepsilon}^{\mathrm{th}}. \tag{5}$$

Moreover $\underline{\varepsilon}_1^{\mathrm{tr}} = 0$, the phase transformation strain tensor is:

$$\underline{\varepsilon}_2^{\mathrm{tr}} = \underline{K}(h_k) \tag{6}$$

where $\underline{K}$ is the traceless ($\mathrm{tr}(\underline{K}) = 0$) eigenstrain associated with the formation of the martensite phase. Thus, it is stipulated that merely eigenstrain $\underline{K}$ depends on internal variables h_k.

Assuming that the total macroscopic strain tensor $\underline{\varepsilon}$ and the total intrinsic strain tensors $\underline{\varepsilon}_\alpha$ must comply with the following relation:

$$\underline{\varepsilon} = (1-\xi)\underline{\varepsilon}_1 + \xi\underline{\varepsilon}_2 \tag{7}$$

The Helmholtz specific free energy function of the two phases system in constrained equilibrium [1] by considering the Eqs. (1), (4) and (7) is

$$\phi(T, \underline{\varepsilon}, \xi, h) = u_0^1 - Ts_0^1 + \frac{1}{2\rho}[\underline{\varepsilon} - \underline{K}\xi - \alpha(t-T_0)\mathbb{I}] : \underline{\underline{L}}[\underline{\varepsilon} - \underline{K}\xi - \alpha(T-T_0)\mathbb{I}] + C_v\left[(T-T_0) - T\ln\frac{T}{T_0}\right] - \xi\pi_0^{\mathrm{f}}(T) + \xi(1-\xi)\phi_{it} \tag{8}$$

where $\pi_0^{\mathrm{f}}(T)$ represents the thermodynamic driving force associated to the phase transformation under stress free state:

$$\pi_0^{\mathrm{f}}(T) = \Delta u_0 - T\Delta s_0 \tag{9}$$

and

$$\Delta u_0 = u_0^1 - u_0^2 \tag{10}$$

$$\Delta s_0 = s_0^1 - s_0^2 \tag{11}$$

represent the difference between internal energy (entropy) of austenite and martensite.

In a classical way, the Cauchy stress tensor can be obtained as

$$\underline{\sigma} = \rho \frac{\partial \phi}{\partial \underline{\varepsilon}} = \underline{\underline{L}}(\underline{\varepsilon} - \underline{\varepsilon}^{\mathrm{tr}} - \underline{\varepsilon}^{\mathrm{th}}) \tag{12}$$

where

$$\underline{\varepsilon}^{\mathrm{tr}} = \underline{K}(h_k)\xi \tag{13}$$

$$\underline{\varepsilon}^{\mathrm{th}} = \alpha(T - T_0)\mathbb{I}. \tag{14}$$

We shall now introduce the concept of "optimum internal arrangements". Raniecki and Lexcellent [1] have established that the set of internal variables h_k minimizes the Helmholtz specific free energy function and the tensor $\underline{K}$ can be derived from a positively homogeneous function of first order g^* ($\underline{\sigma} \mapsto g^*(\underline{\sigma})$). This description allows to take into account the tension compression asymmetry and finally leads to:

$$\underline{\sigma} : \underline{K}(h_k) = \rho g^*(\underline{\sigma}) \tag{15}$$

so

$$\underline{K}(h_k) = \rho \frac{\partial g^*(\underline{\sigma})}{\partial \underline{\sigma}}. \tag{16}$$

The Gibbs potential function g of two phases is defined by

$$g(\underline{\sigma}, T, \xi, h_k) = \phi(\underline{\varepsilon}, T, \xi, h_k) - \frac{\underline{\sigma} : \underline{\varepsilon}}{\rho}. \tag{17}$$

Assuming the expression of ϕ (Eq. (8)), one obtains as an expression of g:

$$\begin{aligned} g(\underline{\sigma}, T, \xi, h_k) = {} & u_0^1 - Ts_0^1 - \xi\pi_0^{\mathrm{f}}(T) + C_v\left[(T - T_0)\right] - T\ln\frac{T}{T_0}\Big] \\ & - \frac{1}{2\rho}\underline{\sigma} : \underline{\underline{L}}^{-1}\underline{\sigma} - \xi g^*(\underline{\sigma}) - \frac{\alpha}{\rho}(T - T_0)\underline{\sigma} \\ & : \underline{Id} + \xi(1 - \xi)\phi_{it}. \end{aligned}$$

Thus, thermal equations of state following from the Eq. (18) are:

- the strain tensor $\underline{\varepsilon}$:

$$\underline{\varepsilon} = -\rho \frac{\partial g}{\partial \underline{\sigma}} = \underline{\underline{L}}^{-1}\underline{\sigma} + \underline{K}\xi + \alpha(T - T_0)\mathbb{I} \tag{18}$$

- the specific entropy s:

$$s = -\frac{\partial g}{\partial T} = s_0^1 - \xi\Delta s_0 + C_v \ln\left(\frac{T}{T_0}\right) + \frac{\alpha}{\rho}\underline{\sigma} : \mathbb{I} \tag{19}$$

- the thermodynamic driving force π_{f}:

$$\pi_{\mathrm{f}}(\underline{\sigma}, T, \xi) = -\frac{\partial g}{\partial \xi} = g^*(\underline{\sigma}) - (1 - 2\xi)\phi_{it} + \pi_0^{\mathrm{f}}(T). \tag{20}$$

These equations form the first group of constitutive equations. One must underline the important strain tensor:

$$\underline{\varepsilon}^{\mathrm{tr}} = \underline{K}(h_k)\xi \tag{21}$$

specially associated with the phase transformation and which takes by time differentiation:

$$\dot{\underline{\varepsilon}}^{\mathrm{tr}} = \dot{\underline{K}}(h_k)\xi + \underline{K}(h_k)\dot{\xi}. \tag{22}$$

For proportional loadings ($\dot{\underline{K}} = 0$) [5], the right term is consistent with a normal phase transformation evolution.

The second law of thermodynamics when written for infinitesimal processes of successive constrained phase equilibria takes the form:

$$\mathrm{d}s + \frac{\mathrm{d}q}{T} = \frac{\mathrm{d}D}{T} \geqslant 0 \tag{23}$$

where $\mathrm{d}q$ and $\mathrm{d}D$ are the incrementals of heat exchange and energy dissipation per unit of mass, respectively. A classical calculation delivers the expression of the increment of dissipation $\mathrm{d}D$ which can not be negative:

$$\mathrm{d}D = \pi_{\mathrm{f}} d\xi \geqslant 0. \tag{24}$$

Thus, the present inequality precludes the forward phase transformation ($\mathrm{A} \to \mathrm{M}$) only if $\pi_{\mathrm{f}} \geqslant 0$ and the reverse only if $\pi_{\mathrm{f}} \leqslant 0$. One has to note that $\pi_{\mathrm{f}} = 0$ implies the equilibrium conditions. The complete set of equations should contain additional kinetics relation for ξ (one for $\mathrm{A} \to \mathrm{M}$ and one another for $\mathrm{M} \to \mathrm{A}$) and will be exposed further in this section.

2.2. Heat equation

It is known that the forward transformation ($\mathrm{A} \to \mathrm{M}$) is exothermal and the reverse transformation ($\mathrm{M} \to \mathrm{A}$) endothermal. Many studies have shown or just taken into account the temperature influence: for dynamic loadings by Collet et al. [6] or for the rate effects loading by Rejzner et al. [7]. In order to quantify the temperature influence on the classical behavior, relations between all of the thermomechanical parameters of the SMA are investigated. First of all, let us consider the energy conservation (Eq. (25)):

$$\rho\dot{u} = \underline{\sigma} : \dot{\underline{\varepsilon}} + r + \mathrm{div}\,\mathbf{q} \tag{25}$$

where u is the internal specific energy, $\mathbf{q}$ is the heat flow vector and r is the internal heat source. Here $\phi = u + Ts$. From the Eq. (25), the expression of the heat equation is thus obtained:

$$C_v\dot{T} + \mathrm{div}\,\mathbf{q} = r + \pi_{\mathrm{f}}(\underline{\sigma}, T, \xi)\dot{\xi} + T\Delta s_0\dot{\xi} - \frac{T\alpha}{\rho}\mathbb{I} : \dot{\underline{\sigma}}. \tag{26}$$

The Fourier's law gives the relation between the heat flow and the temperature:

$$\mathbf{q} = -\lambda\,\mathrm{grad}\,(T) \tag{27}$$

where λ is the conduction coefficient. Assuming this relation, the heat equation becomes:

$$C_v\dot{T} - \lambda\Delta T = r + [\pi_{\mathrm{f}}(\underline{\sigma}, T, \xi) + T\Delta s_0]\dot{\xi} - \frac{T\alpha}{\rho}\mathbb{I} : \dot{\underline{\sigma}} \tag{28}$$

where $\Delta T = T_{,ii}$. Moreover, boundary conditions have to be considered following the different simulations: adiabatic or with imposed external temperature. In a general case, boundary conditions are convection type. The expression given on the boundary domain is written as

$$-\lambda\frac{\partial T}{\partial n} = h(T - T_0) \tag{29}$$

where h is the convection coefficient and $\mathbf{n}$ the outgoing perpendicular vector. One must consider that for an adiabatic simulation: $\mathrm{div}(\mathbf{q}) = 0$ and for major cases, $r = 0$. Thus in this case, the heat equation is reduced to the Eq. (30):

$$C_v\dot{T} = [\pi_f(\underline{\sigma}, T, \xi) + T\Delta s_0]\dot{\xi} - \frac{T\alpha}{\rho}\mathbb{I} : \underline{\dot{\sigma}}. \tag{30}$$

2.3. Equivalent stress and equivalent transformation strain

The main objective of this study is to investigate the pseudoelastic behavior of SMAs under multiaxial proportional loadings. A proportional loading can be interpreted as an uniaxial loading in the equivalent stress–equivalent strain. A definition of an equivalent stress and an equivalent transformation strain is thus required. To do it, we use the transformation domain which has the same role as the yield domain in the elasto-plastic materials. The equation of this yield surface can be written as

$$f_1 = \sigma_{eq} - \sigma_0 = 0 \tag{31}$$

where σ_0 is an offset, and σ_{eq} an equivalent stress to defined and based on the experimental results presented by Bouvet et al. [8,5]. Clearly, an asymmetry between tension and compression is shown into these results. The equivalent Von Mises stress is thus insufficient to describe this phenomenon. We limit ourselves to isotropic SMA, then the equivalent stress depends on the three tensor invariants:

- the hydrostatic pressure $\overline{P}$:

$$\overline{P} = \frac{1}{3}\frac{\mathrm{tr}(\underline{\sigma})}{\bar{\sigma}} \tag{32}$$

- the equivalent Von Mises stress $\bar{\sigma}$:

$$\bar{\sigma} = \left(\frac{3}{2}\mathrm{dev}(\underline{\sigma}) : \mathrm{dev}(\underline{\sigma})\right)^{1/2} \tag{33}$$

- the Lode angle θ between σ_I and $\underline{\sigma}$ the stress direction in the deviatoric stress plane:

$$y_\sigma = \frac{27}{2}\frac{\det(\mathrm{dev}(\underline{\sigma}))}{\bar{\sigma}^3} = \cos(3\theta). \tag{34}$$

Moreover, on can assume that the martensitic transformation of SMA is volume invariant [9] and hence the form of the Eq. (35), independent of the first stress invariant $\overline{P}$ is chosen:

$$\sigma_{eq} = \sigma_{eq}(\bar{\sigma}, y_\sigma) = \bar{\sigma}f(y_\sigma) \tag{35}$$

where the function f allows for the description of the tension– compression asymmetry behavior. For instance: Bouvet et al. [5] have chosen:

$$f(y_\sigma) = \cos\left[\frac{\cos^{-1}(1 - a(1 - y_\sigma))}{3}\right] \tag{36}$$

where a is a material parameter. This expression yields a convex forward phase transformation criterion for all values of a varying within the range $[0, 1]$. The value $a = 0.7$ has been experimentally identified by Bouvet et al. [5] for a CuAlBe SMA sample.

The specific numeric factor occurring in the definition of y_σ normalize this variable such that $|y_\sigma| \leqslant 1$ for all stress states [1]. Many forms of the function f have been already proposed, one can notice these one explicited in [10–12]. The isotropic behavior of two phases RVE and the independence of $\underline{P}$ of the macroscopic eigenstrain $\underline{K}$ imply that the potential g^* is at most function of the stress deviator $\mathrm{dev}(\underline{\sigma})$. Taking into account that g^* is a homogeneous function of order one, we conclude that its general representation may be written in the form:

$$g^*(\underline{\sigma}) = \frac{\gamma}{\rho}\sigma_{eq} \tag{37}$$

where γ is the maximum phase transformation strain in pure shearing. Assuming the Eq. (16), it can be noticed that

$$\underline{K}(h_k) = \gamma\frac{\partial\sigma_{eq}}{\partial\underline{\sigma}}. \tag{38}$$

Thus, one can explicit the expression of $\underline{K}$:

$$\underline{K} = \underline{K}_1 + \underline{K}_2 \tag{39}$$

where

$$\underline{K}_1 = \frac{3}{2}\gamma f(y_\sigma)\underline{N} \tag{40}$$

$$\underline{K}_2 = \frac{9}{2}\gamma f'(y_\sigma)\left(3\underline{N}^2 - y_\sigma\underline{N} - \frac{2}{3}\mathbb{I}\right) \tag{41}$$

with $\underline{N}$ a tensor defined as

$$\underline{N} = \frac{\mathrm{dev}(\underline{\sigma})}{\bar{\sigma}}. \tag{42}$$

The eigenstrain $\underline{K}$ is splitted additively into two parts which are mutually orthogonal in the sense that $\mathrm{tr}(\underline{K}_1\underline{K}_2) = 0$, what follows that $\mathrm{tr}(\underline{K}_2\underline{N}) = 0$.

The fraction of martensite ξ is thus defined by

$$\xi = \frac{\varepsilon_{eq}^{tr}}{\gamma} \tag{43}$$

where ε_{eq}^{tr} is an equivalent transformation strain to be defined. To do it, one must consider the equality between the phase transformation power under proportional loading $\mathscr{P}^{tr}$ and the equivalent transformation power $\mathscr{P}_{eq}^{tr}$ [5]:

$$\underbrace{\underline{\sigma} : \underline{\dot{\varepsilon}}^{tr}}_{\mathscr{P}^{tr}} = \underbrace{\sigma_{eq} : \dot{\varepsilon}_{eq}^{tr}}_{\mathscr{P}_{eq}^{tr}} \tag{44}$$

with this definition, all multiaxial proportional loadings have the same representation in the $(\varepsilon_{eq}^{tr}, \sigma_{eq})$ graph. Denoting the equivalent transformation Von Mises strain $\bar{\varepsilon}^{tr}$ by the Eq. (45):

$$\bar{\varepsilon}^{\mathrm{tr}} = \left(\frac{2}{3}\underline{\varepsilon}^{\mathrm{tr}} : \underline{\varepsilon}^{\mathrm{tr}}\right)^{1/2} \tag{45}$$

an expression of the equivalent transformation strain is thus obtained (Eq. (46)):

$$\varepsilon_{\mathrm{eq}}^{\mathrm{tr}} = \frac{\bar{\varepsilon}^{\mathrm{tr}}}{\sqrt{f^2(y_\sigma) + 9f'^2(y_\sigma)(1-y_\sigma)}}. \tag{46}$$

With this definition, $\varepsilon_{\mathrm{eq}}^{\mathrm{tr}}$ depends on the stress trough y_σ. To avoid this problem, it is possible to calculate y_σ as a function of $\varepsilon^{\mathrm{tr}}$ for every proportional loading path. But, this function can not be analytically determined, and an approximation defined by the Eq. (47) is used:

$$\frac{1}{\sqrt{f^2(y_\sigma) + 9f'^2(y_\sigma)(1-y_\sigma)}} \approx \frac{f(-y_\varepsilon)}{f(-1)} \tag{47}$$

where y_ε is the third strain tensor invariant:

$$y_\varepsilon = 4\frac{\det(\underline{\varepsilon}^{\mathrm{tr}})}{(\bar{\varepsilon}^{\mathrm{tr}})^3}. \tag{48}$$

2.4. Kinetic laws

The inequality of Clausius–Duhem precludes the forward phase transformation only if $\pi^{\mathrm{f}} \geqslant 0$ and the reverse one if $\pi^{\mathrm{f}} \leqslant 0$. One has to note that $\pi^{\mathrm{f}} = 0$ implies the equilibrium condition. Thus it does not exist any thermodynamic relation giving the hysteresis loop branches equations. Nevertheless, such equations are needed to determine the evolution laws of the fraction of martensite ξ. In order to specify the kinetic equations driving the phase transformation, it can be presumed the existence of two functions $\psi^\alpha(\pi^{\mathrm{f}}, \xi)$ $(\alpha = 1, 2)$ such that an active process of parent phase decomposition $(\mathrm{A} \to \mathrm{M}{:}\mathrm{d}\xi > 0)$ can only proceed when $\psi^1 = \text{const}$, $(\mathrm{d}\psi^1 = 0)$ and an active process of martensite decomposition $(\mathrm{M} \to \mathrm{A}{:}\mathrm{d}\xi < 0)$ can only proceed if $\psi^2 = \text{const}$, $(\mathrm{d}\psi^2 = 0)$. These yield functions are chosen as

$$\psi^1 = \pi^{\mathrm{f}} - k^{(1)}(\xi) \tag{49}$$

$$\psi^2 = -\pi^{\mathrm{f}} + k^{(2)}(\xi). \tag{50}$$

The expression of $k^\alpha(\xi)$ are built to give kinetics in agreement with the measurements of metallurgists as Koistinen and Marbuger [13]:

$$k^{(1)}(\xi) = -A_1 \ln(1-\xi) \tag{51}$$

$$k^{(2)}(\xi) = A_2 \ln(\xi). \tag{52}$$

with

$$A_1 = \frac{\Delta s_0 - \bar{s}_0}{a_1}, \quad A_2 = \frac{\Delta s_0 + \bar{s}_0}{a_2} \tag{53}$$

The coefficient a_1 and a_2 can be obtained with the condition $\psi^\alpha = 0$ for stress free state. They can be written as

$$a_1 = \frac{-\ln(1-\xi_{\mathrm{f}}^{\mathrm{M}})}{M_{\mathrm{s}}^0 - M_{\mathrm{f}}^0}, \quad a_2 = \frac{-\ln(\xi_{\mathrm{f}}^{\mathrm{A}})}{A_{\mathrm{f}}^0 - A_{\mathrm{s}}^0} \tag{54}$$

Commonly used values for the forward and reverse transformations are respectively $\xi_{\mathrm{f}}^{\mathrm{M}} = 0.99$ and $\xi_{\mathrm{f}}^{\mathrm{A}} = 0.01$. Thanks to derivation, the kinetic laws for forward and reverse phase transformations are obtained:

$$\dot{\xi}_{\mathrm{A}\to\mathrm{M}}(\dot{\sigma}_{\mathrm{eq}}, \xi, \dot{T}) = \frac{\frac{\gamma\dot{\sigma}_{\mathrm{eq}}}{\rho} - \Delta s_0 \dot{T}}{\frac{A_1}{1-\xi} - 2\phi_{it}}, \tag{55}$$

$$\dot{\xi}_{\mathrm{M}\to\mathrm{A}}(\dot{\sigma}_{\mathrm{eq}}, \xi, \dot{T}) = \frac{\frac{\gamma\dot{\sigma}_{\mathrm{eq}}}{\rho} - \Delta s_0 \dot{T}}{\frac{A_2}{\xi} - 2\phi_{it}}. \tag{56}$$

2.5. Assessment of the equations set

An assessment of all the model equations developed in this section is yet done:

- the equivalent Von Mises stress $\bar{\sigma}$:

$$\bar{\sigma} = \left(\frac{3}{2}\mathrm{dev}(\underline{\sigma}) : \mathrm{dev}(\underline{\sigma})\right)^{1/2} \tag{57}$$

- the equivalent Von Mises strain $\bar{\varepsilon}$:

$$\bar{\varepsilon} = \left(\frac{2}{3}\mathrm{dev}(\underline{\varepsilon}) : \mathrm{dev}(\underline{\varepsilon})\right)^{1/2} \tag{58}$$

- the quantity y_σ:

$$y_\sigma = \frac{27}{2}\frac{\det(\mathrm{dev}(\underline{\sigma}))}{\bar{\sigma}^3} \tag{59}$$

- the function f:

$$f(y_\sigma) = \cos\left[\frac{\cos^{-1}(1 - a(1-y_\sigma))}{3}\right] \tag{60}$$

- the equivalent stress σ_{eq}:

$$\sigma_{\mathrm{eq}}(\bar{\sigma}, y_\sigma) = \bar{\sigma} f(y_\sigma) \tag{61}$$

- the equivalent transformation strain $\varepsilon_{\mathrm{eq}}^{\mathrm{tr}}$:

$$\varepsilon_{\mathrm{eq}}^{\mathrm{tr}} = \frac{\bar{\varepsilon}^{\mathrm{tr}}}{\sqrt{f^2(y_\sigma) + 9f'^2(y_\sigma)(1-y_\sigma)}} \tag{62}$$

- the tensor $\underline{N}$:

$$\underline{N} = \frac{\mathrm{dev}\underline{\sigma}}{\bar{\sigma}} \tag{63}$$

- the eigenstrain $\underline{K}$:

$$\underline{K} = \frac{3}{2}\gamma f(y_\sigma)\underline{N} + \frac{9}{2}\gamma f'(y_\sigma)\left(3N^2 - y_\sigma \underline{N} - \frac{2}{3}\mathbb{I}\right) \tag{64}$$

- the transformation strain tensor $\underline{\varepsilon}^{\mathrm{tr}}$:

$$\underline{\varepsilon}^{\mathrm{tr}} = \underline{K}(h_k)\xi \tag{65}$$

- the thermal strain tensor $\underline{\varepsilon}^{\mathrm{th}}$:

$$\underline{\varepsilon}^{\mathrm{th}} = \alpha(T - T_0)\mathbb{I} \tag{66}$$

- the thermodynamic driving force π_{f}:

$$\pi_{\mathrm{f}}(\sigma_{\mathrm{eq}}, T, \xi) = \frac{\gamma\sigma_{\mathrm{eq}}}{\rho} + \pi_0^{\mathrm{f}}(T) - (1-2\xi)\phi_{it} \tag{67}$$

- the stress tensor $\underline{\sigma}$:

$$\underline{\sigma} = \underline{\underline{L}}(\underline{\varepsilon} - \underline{K}\xi - \alpha(T - T_0)\mathbb{I}) \tag{68}$$

- the heat equation:

$$C_v\dot{T} - \lambda\Delta T = r + \pi_f(\sigma_{eq}, T, \xi)\dot{\xi} + T\Delta s_0\dot{\xi} - \frac{T\alpha}{\rho}\mathbb{I} : \dot{\underline{\sigma}} \tag{69}$$

- the boundary thermal condition associated to an external imposed temperature:

$$\frac{\partial T}{\partial n} = -\frac{h}{\lambda}(T - T0) \tag{70}$$

- the kinetic laws:

$$\dot{\xi}_{A\to M}(\dot{\sigma}_{eq}, \xi, \dot{T}) = \frac{\frac{\gamma\dot{\sigma}_{eq}}{\rho} - \Delta s_0\dot{T}}{\frac{A_1}{1-\xi} - 2\phi_{it}}, \tag{71}$$

$$\dot{\xi}_{M\to A}(\dot{\sigma}_{eq}, \xi, \dot{T}) = \frac{\frac{\gamma\dot{\sigma}_{eq}}{\rho} - \Delta s_0\dot{T}}{\frac{A_2}{\xi} - 2\phi_{it}}. \tag{72}$$

3. Implementation in COMSOL©

COMSOL© is a modeling package for the simulation of any physical process and can be described with partial differential equations (PDEs). It features state-of-the-art solvers that address complex problems quickly and accurately, while its intuitive structure is designed to provide ease of use and flexibility. This software is chosen for its ability to build automatically some cycles and internal loops. The R_L model described in the previous section has been implemented for 2D problems with plane stress assumptions. It can be assimilated to a multiphysic coupled problem between the structural mechanic module (for the mechanic behavior) and the PDEs module (for the kinetic transformations).

This section resumes the "translation" of the R_L model for plane stress problems into characteristic equations to be implemented in COMSOL©.

3.1. Principle of virtual work

The principle of virtual work expressed in global stress components states that the sum of virtual works from internal strains are equal to works from external loads. This principle will be applied under the assumption of small disturbances.

Let us consider a continuous domain Ω as it is shown on the Fig. 1, loaded in force $\overline{F}/\Gamma_t$ or in displacement $\overline{U_0}/\Gamma_u$. $\bar{\mathbf{f}}$ represents the volumic force and $\bar{n}$ the outgoing perpendicular vector. The total stored energy $\mathscr{W}$ from external and internal strains and loads is:

$$\mathscr{W}(\mathbf{u}^*) = -\frac{1}{2}\int_\Omega \mathrm{tr}\underline{\sigma} \cdot \underline{\varepsilon}(\mathbf{u}^*)]\mathrm{d}\Omega + \int_\Omega \bar{\mathbf{f}}^* \cdot \mathbf{u}^*\,\mathrm{d}\Omega + \int_{\Gamma_t} \overline{\mathbf{F}} \cdot \mathbf{u}^*\,\mathrm{d}\Omega \tag{73}$$

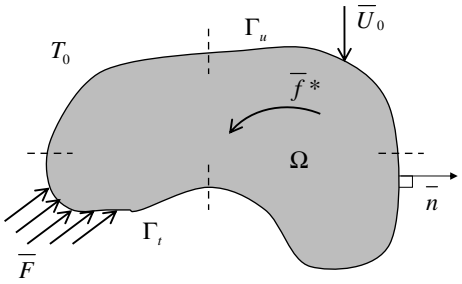

Fig. 1. Domain Ω and boundary conditions.

where $\bar{\mathbf{f}}^*$ is defined in function of the acceleration $\bar{\gamma}$ and $\bar{\mathbf{f}}$ as

$$\bar{\mathbf{f}}^* = \bar{\mathbf{f}} - \rho \cdot \bar{\gamma} \tag{74}$$

and $\mathbf{u}^*$ belongs to the whole of the kinematically admissible fields defined by

$$\mathscr{U}_{ad} = \{\mathbf{u}^* \in H_1/\mathbf{u}^* = \overline{\mathbf{U}}_0 \quad \text{on } \Gamma_u\} \tag{75}$$

and

$$\underline{\sigma}(\mathbf{n}) = \overline{\mathbf{F}} \quad \text{on } \Gamma_t. \tag{76}$$

Thus, the principal of virtual work states that

$$\mathrm{d}\mathscr{W} = 0. \tag{77}$$

3.2. Implementation

In order to calculate $\mathscr{W}$, the stress tensor $\underline{\sigma}$, solution of the multiphysic problem must be evaluated in the COMSOL© scalar expressions. This can be done by considering the Eq. (77). One can note that the thermal strain $\underline{\varepsilon}^{th}$ in the expression of $\underline{\sigma}$ is neglected.

$$\underline{\sigma} = \underline{\underline{L}}(\underline{\varepsilon}(\mathbf{u}) - \underline{K}(\underline{\sigma})\xi). \tag{78}$$

The Eq. (78) appears as an implicit expression of $\underline{\sigma}$, ($\underline{\sigma} = f(\underline{\varepsilon}(\mathbf{u}), \underline{\sigma})$), which is incomprehensible by COMSOL©. The value of K_{ij} depends on the boundary conditions, loadings and finally the investigated problem.

In the case of force loadings (displacement loadings), a tensor $\widetilde{\underline{K}}$ is obtained by the elastic resolution of the Neumann's problem (Dirichlet's problem). This elastic resolution is typically done by a "structural mechanic module" called "PS1".

If $(\tilde{\underline{\sigma}}, \tilde{\underline{\varepsilon}})$ is the elastic solution obtained by this module, the Eq. (78) becomes:

$$\underline{\sigma} = \underline{\underline{L}}(\underline{\varepsilon}(\mathbf{u}) - \widetilde{\underline{K}}\xi) \tag{79}$$

where

$$\widetilde{\underline{K}} = \frac{3}{2}\gamma f(\tilde{y}_\sigma)\widetilde{\underline{N}} + \frac{9}{2}\gamma f'(\tilde{y}_\sigma)\left(3\widetilde{N}^2 - \tilde{y}_\sigma\widetilde{\underline{N}} - \frac{2}{3}\mathbb{I}\right) \tag{80}$$

and

$$\tilde{y}_\sigma = \frac{27}{2}\frac{\det(\mathrm{dev}(\tilde{\underline{\sigma}}))}{\tilde{\bar{\sigma}}^3}, \quad \widetilde{N} = \frac{\mathrm{dev}(\tilde{\sigma})}{\tilde{\bar{\sigma}}} \tag{81}$$

By this way, the implicit problem (Eq. (78)) is transformed into the explicit problem (Eq. (79)), which is easily implemented in COMSOL©.

Finally, four modules are used to solve the multiphysic problem:

- "structural mechanic 1" (PS1): elastic resolution, construction of the components $\tilde{K}_{ij}$ of $\underline{\tilde{K}}$,
- "structural mechanic 2" (PS2): nonlinear resolution, construction of the multiphysic problem where the solution is $\underline{\sigma}$ and **u**,
- "partial differential equation 1" (PDEs1): nonlinear coupling with PS2. Calculation of the increment or decrement of ξ,
- "partial differential equation 2" (PDEs2): nonlinear coupling with PS2 and PDEs1. Integration of the heat equation, calculation of the temperature T.

The diagram given on Fig. 2 shows the interactions between these four modules.

The computation of $\underline{\tilde{K}}$ and ξ (at each time of the process) gives $\underline{\varepsilon}^{tr}$ and allows the nonlinear resolution of the Eq. (77).

3.3. Case of the plane stress

By considering the plane stress assumptions (corresponding to a plate under "ad hoc" loading conditions), the stress tensor is clearly defined by

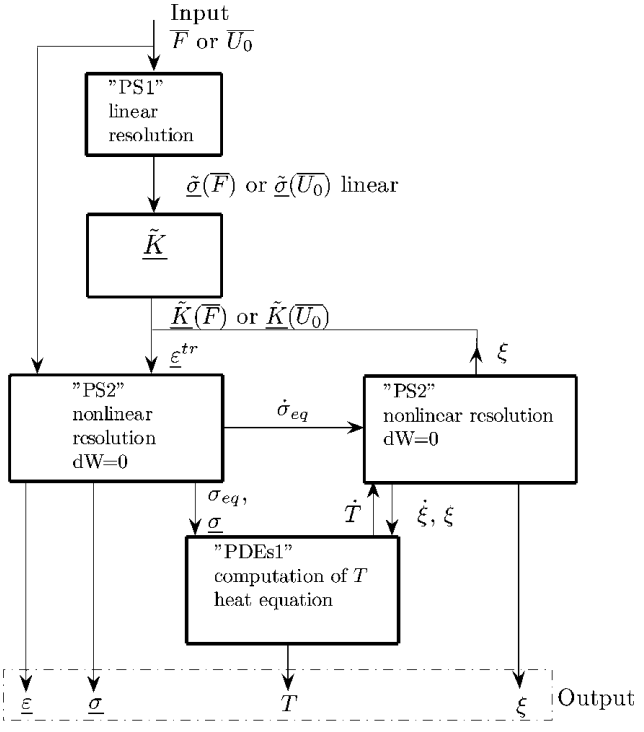

Fig. 2. Diagram of the interactions between the four modules "PS1", "PS2", "PDEs1" and "PDEs2".

$$\underline{\sigma} = \begin{bmatrix} \sigma_{11} & \sigma_{12} & 0 \\ \sigma_{12} & \sigma_{22} & 0 \\ 0 & 0 & 0 \end{bmatrix}. \tag{82}$$

Thus, $\tilde{y}_\sigma$ can be explicited as

$$\tilde{y}_\sigma = \frac{1}{\tilde{\bar{\sigma}}^3}(\tilde{\sigma}_{11}^3 + \tilde{\sigma}_{22}^3 + 9/2(\tilde{\sigma}_{22} + \tilde{\sigma}_{11})\tilde{\sigma}_{12}^2 - 3/2(\tilde{\sigma}_{11}^2\tilde{\sigma}_{22} + \tilde{\sigma}_{22}^2\tilde{\sigma}_{11})) \tag{83}$$

with the equivalent Von Mises stress:

$$\tilde{\bar{\sigma}} = (\tilde{\sigma}_{11}^2 + \tilde{\sigma}_{22}^2 + 3\tilde{\sigma}_{12}^2 - \tilde{\sigma}_{11}\tilde{\sigma}_{12})^{1/2}. \tag{84}$$

Assuming this definition of $\bar{\sigma}$, the tensor $\underline{K}$ components can be explicited as

Table 1
Constants for NiTi alloy (1)

Phase transformation temperature			
Designation	Notation	Value	Unit
Austenite start	A_s^0	247	K
Austenite finish	A_f^0	279	K
Martensite start	M_s^0	275	K
Martensite finish	M_f^0	209	K

Table 2
Constants for NiTi alloy (2)

Material parameters			
Designation	Notation	Value	Unit
Young's modulus	E	52×10^9	Pa
Poisson's ratio	ν	0.3	∅
Density	ρ	6500	kg m^{-3}
Internal energy difference	Δu_0	8909	J kg^{-1}
Internal entropy difference	Δs_0	46	J kg^{-1} K^{-1}
Coherence internal energy	$\bar{u}_0$	461.5	J kg^{-1}
Coherence internal entropy	$\bar{s}_0$	0	J kg^{-1}
Equivalent eigenstrain	γ	6%	∅
Thermal dilatation coefficient	α	11×10^{-6}	K^{-1}
Conduction coefficient	λ	56.5	W m^{-1} K^{-1}
Convection coefficient	h	5	W m^{-2} K^{-1}
Specific heat	C_v	480	J K kg^{-1}
Coefficient A_1	A_1	699	J kg^{-1}
Coefficient A_2	A_2	280	J kg^{-1}
Asymmetry parameter a	a	0.7	∅

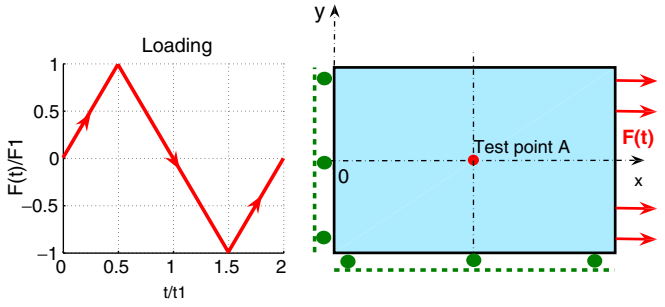

Fig. 3. Force loading and boundary conditions for a plate in tension.

$$\widetilde{K}_{11} = 3/2\gamma f(\tilde{y}_\sigma)\widetilde{N}_{11} + 9/2\gamma f'(\tilde{y}_\sigma)(3(\widetilde{N}_{11}^2 + \widetilde{N}_{12}^2) - \tilde{y}_\sigma \widetilde{N}_{11} - 2/3) \quad (85)$$

$$\widetilde{K}_{22} = 3/2\gamma f(\tilde{y}_\sigma)\widetilde{N}_{22} + 9/2\gamma f'(\tilde{y}_\sigma)(3(\widetilde{N}_{22}^2 + \widetilde{N}_{12}^2) - \tilde{y}_\sigma \widetilde{N}_{22} - 2/3) \quad (86)$$

$$\widetilde{K}_{33} = 3/2\gamma f(\tilde{y}_\sigma)\widetilde{N}_{33} + 9/2\gamma f'(\tilde{y}_\sigma)(3\widetilde{N}_{33}^2 - \tilde{y}_\sigma \widetilde{N}_{33} - 2/3) \quad (87)$$

$$\widetilde{K}_{12} = 3/2\gamma f(\tilde{y}_\sigma)\widetilde{N}_{33} + 9/2\gamma f'(\tilde{y}_\sigma)(3\widetilde{N}_{12}(N_{11} + \widetilde{N}_{22}) - \tilde{y}_\sigma \widetilde{N}_{12}) \quad (88)$$

and with the definition of the tensor $\underline{N}$:

$$\underline{\widetilde{N}} = \frac{1}{\tilde{\bar{\sigma}}} \begin{bmatrix} \frac{2\tilde{\sigma}_{11} - \tilde{\sigma}_{22}}{3} & \tilde{\sigma}_{12} & 0 \\ \tilde{\sigma}_{12} & \frac{-\tilde{\sigma}_{11} + 2\tilde{\sigma}_{22}}{3} & 0 \\ 0 & 0 & -\frac{\tilde{\sigma}_{11} + \tilde{\sigma}_{22}}{3} \end{bmatrix}. \quad (89)$$

The explicit heat equation expression is written:

$$C_v \dot{T} - \lambda \Delta T = r + \pi_f(\sigma_{eq}, T, \xi)\dot{\xi} + T\Delta s_0 \dot{\xi} - \frac{T\alpha}{\rho}(\dot{\sigma}_{11} + \dot{\sigma}_{22}). \quad (90)$$

Assuming the plane stress assumptions, the strain tensor expression is given by

$$\underline{\varepsilon} = \begin{bmatrix} \varepsilon_{11} & \varepsilon_{12} & 0 \\ \varepsilon_{12} & \varepsilon_{22} & 0 \\ 0 & 0 & \varepsilon_{33} \end{bmatrix}. \quad (91)$$

The partition of the total strain in elastic part and phase transformation part is recalled:

$$\underline{\varepsilon} = \underline{\varepsilon}^{el} + \underline{\varepsilon}^{tr} \quad (92)$$

and the elastic strain tensor can be clarified as

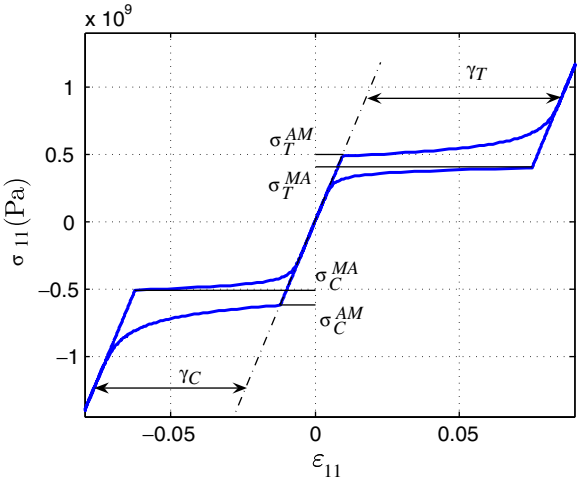

Fig. 4. Illustration of the isothermal relationship between uniaxial stress and strain (pseudoelasticity: $T > A_f^0$).

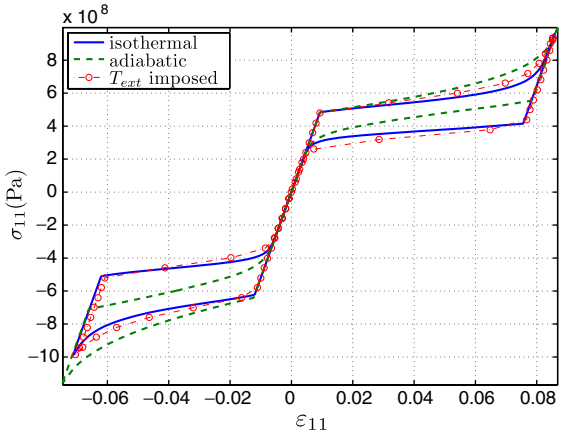

Fig. 5. Illustration of the uniaxial stress σ_{11} in function of the uniaxial strain ε_{11} for isothermal adiabatic and imposed external temperature at the test point A.

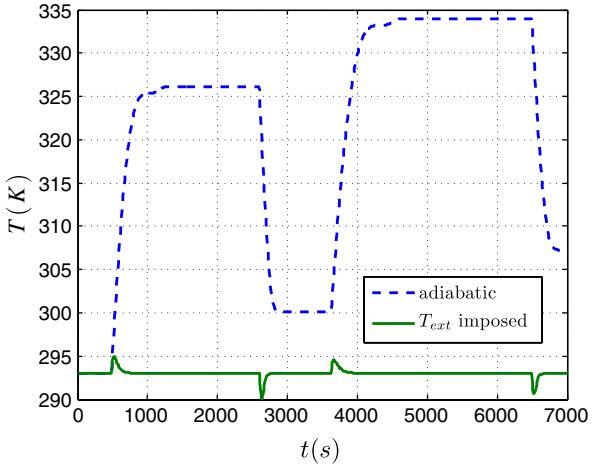

Fig. 6. Evolution of the temperature T in function of the time t at the test point A.

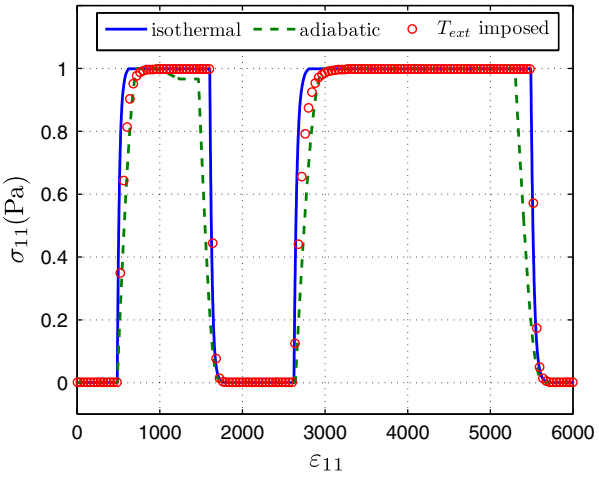

Fig. 7. Evolution of the fraction of martensite ξ in function of the time t at the test point A.

$$\underline{\varepsilon}^{el} = \begin{bmatrix} \varepsilon_{11} - \widetilde{K}_{11}\xi & \varepsilon_{12} - \widetilde{K}_{12}\xi & 0 \\ \varepsilon_{12} - \widetilde{K}_{12}\xi & \varepsilon_{22} - \widetilde{K}_{22}\xi & 0 \\ 0 & 0 & \varepsilon_{33}^{el} \end{bmatrix} \tag{93}$$

with

$$\varepsilon_{33}^{el} = -\frac{v}{1-v}(\varepsilon_{11}^{el} + \varepsilon_{22}^{el}). \tag{94}$$

The equivalent Von Mises strain can be explicited as

$$\bar{\varepsilon} = \frac{2}{3}(\varepsilon_{11}^2 + \varepsilon_{22}^2 + \varepsilon_{33}^2 + 3\varepsilon_{12}^2 - \varepsilon_{11}\varepsilon_{22} - \varepsilon_{11}\varepsilon_{33} - \varepsilon_{22}\varepsilon_{33})^{1/2}. \tag{95}$$

and the equivalent transformation Von Mises strain:

$$\bar{\varepsilon}_{tr} = \frac{2}{3}(\varepsilon_{11_{tr}}^2 + \varepsilon_{22_{tr}}^2 + \varepsilon_{33_{tr}}^2 + 3\varepsilon_{12_{tr}}^2 - \varepsilon_{11_{tr}}\varepsilon_{22_{tr}} - \varepsilon_{11_{tr}}\varepsilon_{33_{tr}} - \varepsilon_{22_{tr}}\varepsilon_{33_{tr}})^{1/2}. \tag{96}$$

The quantity y_ε is thus explicited as

$$y_\varepsilon = 4\frac{\varepsilon_{11_{tr}}\varepsilon_{22_{tr}}\varepsilon_{33_{tr}} - \varepsilon_{12_{tr}}^2\varepsilon_{33_{tr}}}{\bar{\varepsilon}_{tr}}. \tag{97}$$

3.4. Model constants for NiTi alloy

The composition of the SMA used in the numerical application is NiTi. Its characteristics phase transformation and material parameters are indexed in the Tables 1 and 2. These parameters have been identified by performing classical tensile tests at different temperature in the range of plasticity as described in [1,7,2].

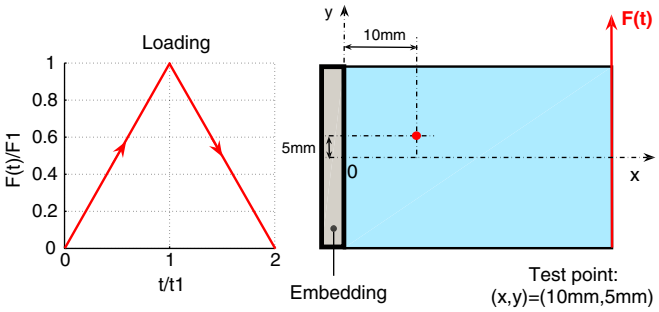

Fig. 8. Force loading: plate in bending loaded in its plane.

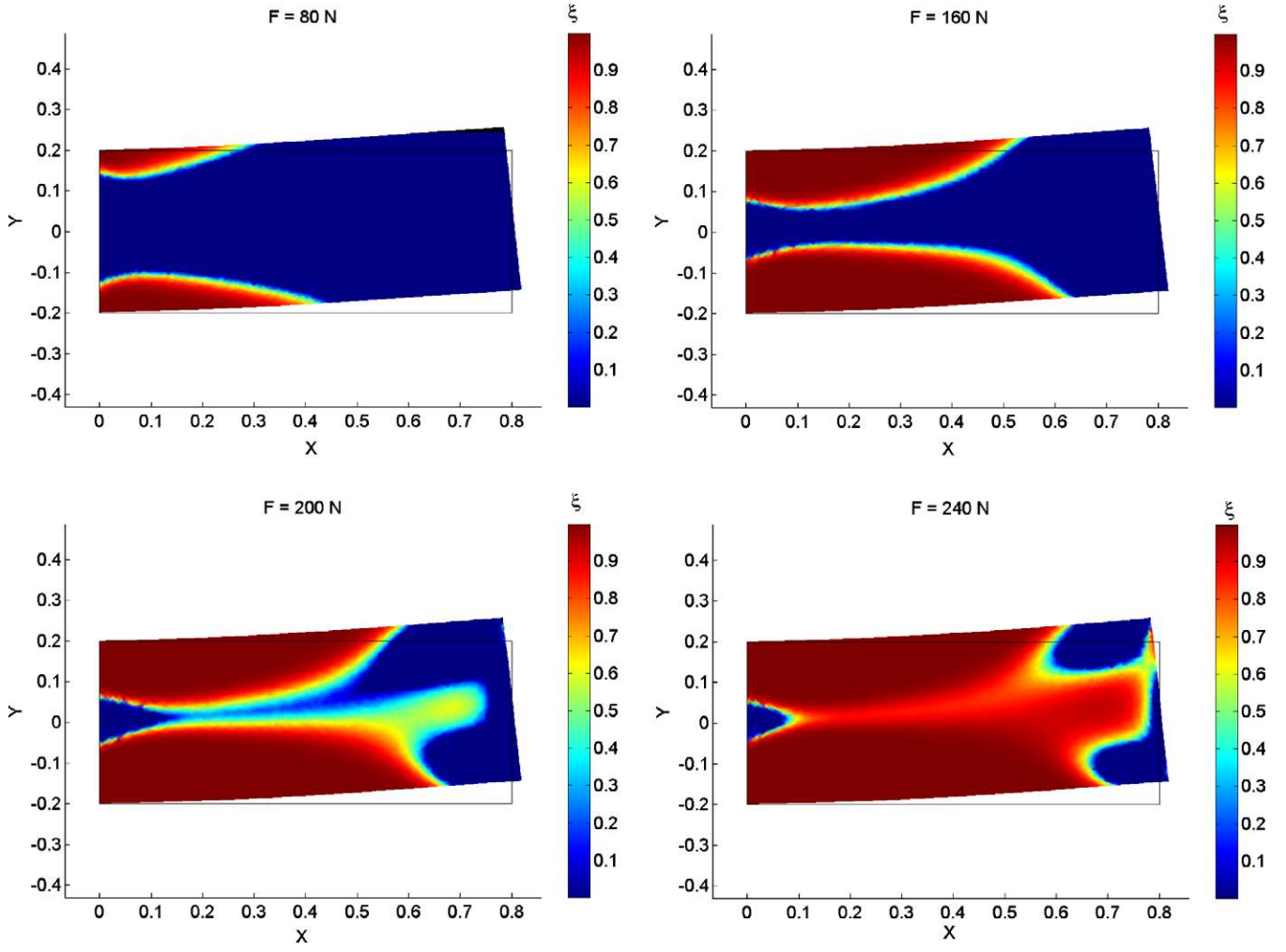

Fig. 9. Ratio ξ of martensite on the plate.

4. Results

In order to validate the implementation presented in the previous section, many static tests were performed. One homogeneous and one nonhomogeneous test are presented: a plate in tension and a plate in bending loaded in its plane. These tests are performed for a rectangular plate. Its dimensions are:

- length: $L = 80$ mm,
- width: $l = 40$ mm,
- thickness: $e = 2$ mm.

For both tests, three implementation are performed: isothermal ($T(x, y) = T_0$), adiabatic ($\mathbf{q} = 0$) and with an external imposed temperature: ($T_{ext} = T_0$).

4.1. Plate in tension

As it is shown in the Fig. 3, a plate is loaded in force for a tension–compression cycle in order to observe the forward and reverse transformation.

The normal stress σ_{11} isothermal evolution in function of the normal strain ε_{11} is given at the test point A on the Fig. 4.

Raniecki et al. [1] have established the following conclusions:

- the critical stress for the forward transformation in tension σ_T^{AM} is smaller than the absolute value of corresponding critical stress $\sigma_C^{AM} < 0$ in compression:

$$\sigma_T^{AM} < -\sigma_C^{AM} \tag{98}$$

on the Fig. 4, one can notice that $\sigma_T^{AM} = 4.8 \times 10^8$ Pa and $\sigma_C^{AM} = -6.2 \times 10^8$ Pa, thus the relation (98) is quite verified.

- the pseudoelastic amplitude γ_T in tension is greater than the one found in compression say γ_C. However, the energies in tension and compression represented by product of critical stress and pseudoelastic amplitude are the same:

$$\gamma_T > \gamma_C \tag{99}$$

$$\sigma_T^{AM}\gamma_T = |\sigma_C^{AM}|\gamma_C \tag{100}$$

The marksheet on the Fig. 4 gives: $\gamma_T = 0.0675$, $\gamma_C = 0.0529$. Thus one can calculates $\sigma_T^{AM}\gamma_T = 328\times\ 10^5$ Pa and $|\sigma_C^{AM}|\gamma_C = 324 \times 10^5$ Pa. Both Eqs. (99) and (100) are verified.

The normal stress σ_{11} evolution versus the normal strain ε_{11} is given at the test point A on the Fig. 5 for isothermal, adiabatic and external imposed temperature.

The temperature evolution in function of the time t is given at the test point A on the Fig. 6.

For the adiabatic case, the SMA cannot evacuate the calories. Thus, an increase (decrease) of the temperature is noticed for the forward (reverse) transformation. Raniecki et al. [1] have shown an increase of the stress with an increase of the temperature. It can be noticed that for the adiabatic case. The pseudoelastic adiabatic stress is more important as the isothermal stress for a fixed strain (Fig. 6).

For the external imposed temperature case, the SMA can evacuate the calories. Thus, the increase (decrease) of the temperature is quickly stopped by this convection thermal transfer. And, finally, the SMA temperature is practically equal to T_0.

For a fixed given strain, the external imposed stress is thus between the isothermal stress and the adiabatic stress. The evolution of the fraction of martensite ξ in function of the time t is given at the test point A on the Fig. 7. One can assume that the fraction of martensite evolution is faster with the temperature evolution.

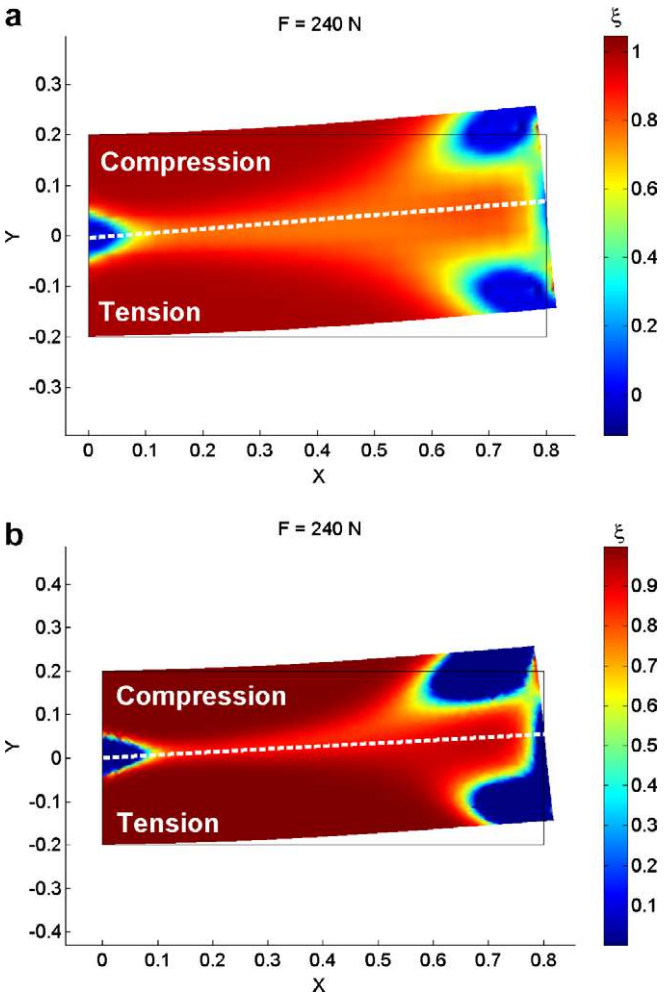

Fig. 10. Force loading plate ratio of martensite ξ on the plate in both cases of the symmetrical model [2] and the asymmetric model [1].

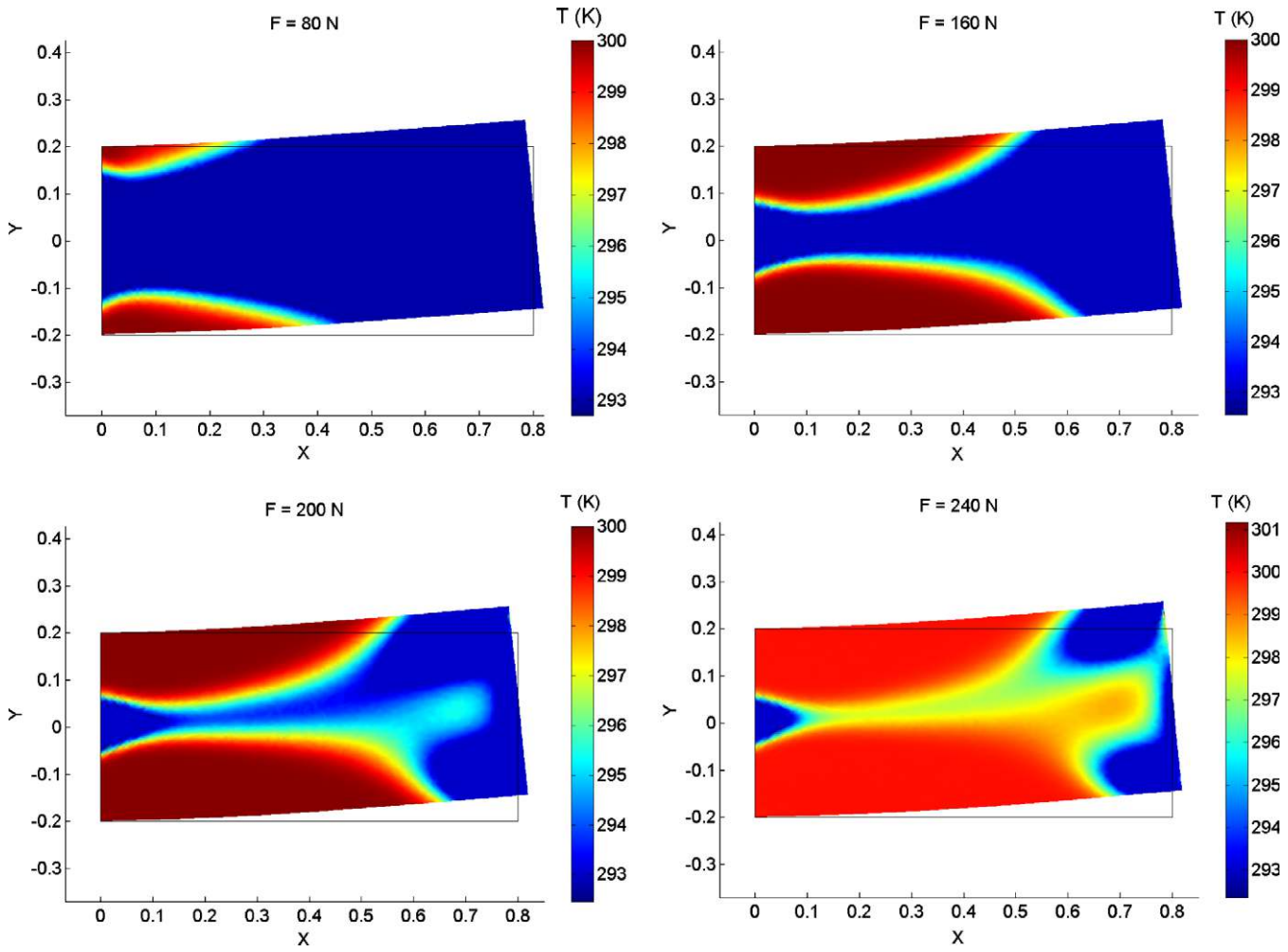

Fig. 11. Adiabatic simulations: temperature T on the plate.

4.2. Plate in bending loaded in its plane

A plate in bending loaded in its plane (Fig. 8) is now performed. this is a nonhomogeneous test. The aim of this simulation is to observe different ratios of martensite and the temperature evolution inside the plate. The volume fraction of martensite depends on the location on the plate.

The four figures in Fig. 9 show for an isothermal simulation the appearance of the martensite and thus the disappearance of the austenite during the load phase. It clearly show that the martensite ratio repartition is not symmetrical compared to the $(0, \overrightarrow{x})$ axis. A simulation with the symmetrical model developed in 1992 by Raniecki et al. [2] is compared with the one [1] recalled in the Section 2.1. For the same material properties and force loading level, the Fig. 10 represents the martensite ratio repartition for both modelisations in the case of the plate loaded in its plane. The upper part of the plate works in tension while the lower part of the plate works in compression. Thus, the asymmetry tension–compression clearly appears: The martensite ratio repartition is symmetric with the [2] implementation (Fig. 10a) compared to the $(0, \overrightarrow{x})$ axis and asymmetrical with the [1] implementation (Fig. 10b).

For the adiabatic case, a temperature increase is shown. This phenomenon is predicted in [1]. The following figures (Fig. 11) represent the temperature on the plate for different values of loading F.

As it is the same case for the adiabatic implementation of a plate in tension, the SMA cannot evacuate the calories for this present simulation. Thus, an increase of temperature is notice and it is evaluated as seven degrees (293 K $\rightarrow$ 300 K). On these previous figures (Fig. 11), one can check that the temperature increase with the fraction volume of martensite increase. Thus, these simulations confirms that the temperature evolution is due to the martensitic transformation: the forward transformation (A $\rightarrow$ M) is exothermic and the reverse transformation (M $\rightarrow$ A) endothermic.

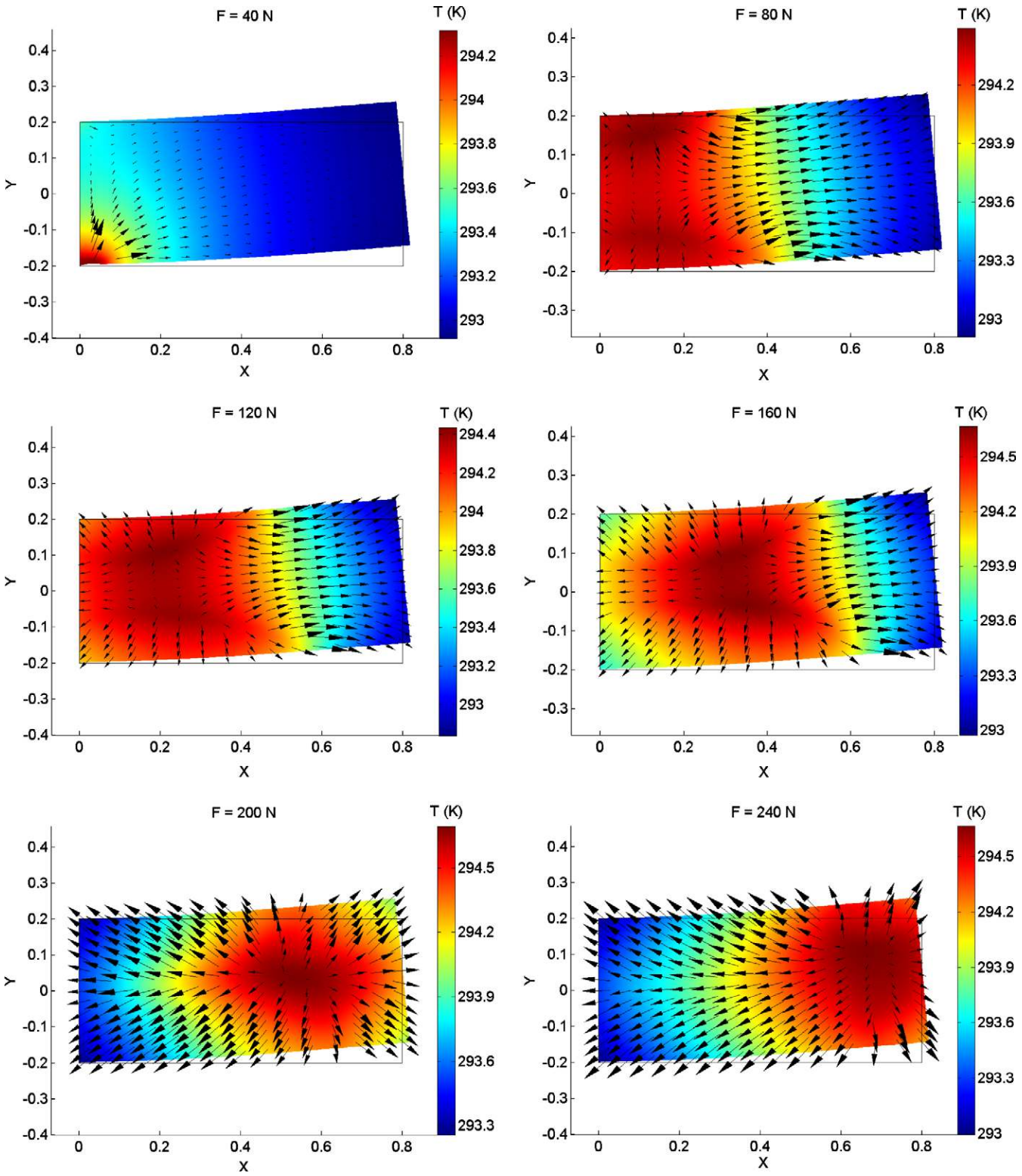

Fig. 12. With an external imposed temperature simulation: temperature T on the plate and heat flow.

At least, a test with an external imposed temperature is presented. As previously, the following figures (Fig. 12) show the temperature and the heat flow (arrows) on the plate.

Let us consider a test point A(x,y) located at the position ($x = 10$ mm, $y = 5$ mm) as it is shown on the Fig. 8. At this point, the material response is thus given in the $(\varepsilon_{\mathrm{eq}}^{\mathrm{tr}}, \sigma_{\mathrm{eq}})$ plane (Fig. 13).

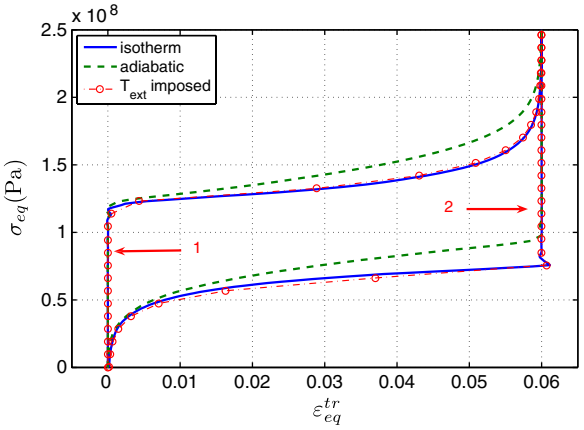

Fig. 13. Force loading: plate in bending loaded in its plane, evolution of the equivalent stress σ_{eq} in function of the equivalent transformation strain ε_{eq}^{tr} for the three isothermal, adiabatic and imposed external temperature cases.

The typical pseudoelastic behavior is obtained for isothermal, adiabatic and with imposed external temperature. One can notice that there's no equivalent transformation strain for both elastic behavior of austenite and martensite. (details 1 and 2 on the Fig. 13).

4.3. Rate effects

In 2000, Lexcellent and Rejzner [14] clearly show that the rate loading effects are not negligible because it induces a continuous change of the actual temperature of the SMA sample. The change in temperature linked to the strain rate or during creep or relaxation is evaluated by the integration of the heat equation.

Previously, the experiments performed by Lim and Mcdowell [15] in 1999 on thin NiTi tubes shown that during phase transformation latent heat will be released/absorbed and the temperature history and coupled transformation driving force depend on the rate of the applied loading relative to heat transfer to or away from the specimen gage section.

The thermodynamical model with external imposed temperature written in the Section 2.1 is able to confirm these rate effects. To do it, let us consider the plate in tension presented in the Section 4.1. The plate is loaded in force with three different force rates (with section area equal to 8×10^{-4} m):

- $\dot{F}_1 = 0.04$ N s^{-1}
- $\dot{F}_2 = 0.4$ N s^{-1}
- $\dot{F}_3 = 4$ N s^{-1}

The material response is given in the following Fig. 14 in the $(\varepsilon_{11}, \sigma_{11})$ plane.

One can notice that the pseudoelastic behavior of the SMA is clearly influenced by the force loading rate. This results confirms the investigations results exposed in

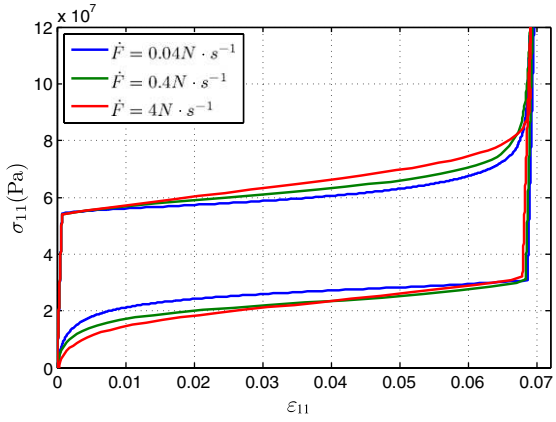

Fig. 14. Force loading: plate in tension, evolution of the normal stress σ_{11} in function of the normal strain ε_{11} for different force rates loading.

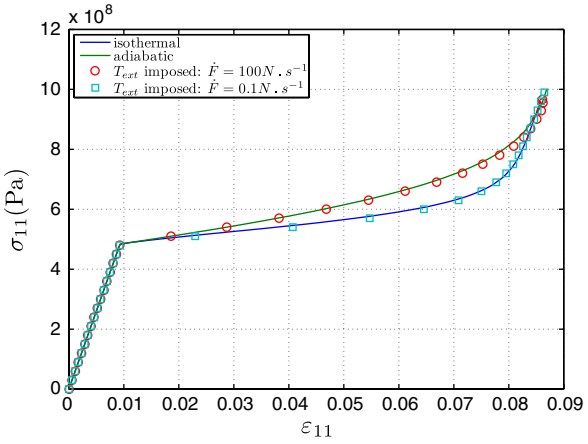

Fig. 15. Force loading: plate in tension, evolution of the normal stress σ_{11} in function of the normal strain ε_{11} for both high and slow force rates loading. Comparison with adiabatic and isothermal simulations.

[14,15]. Typically, a slow rate loading test can be assimilated as a quasi static test. Thus, the SMA sample keep the temperature constant during this test. Hence, an external imposed temperature test with a high rate loading can be assimilated as an isothermal test. In the same way, an external imposed temperature test with a high rate loading can be assimilated as an adiabatic test: the heat transfer between the external field and the SMA sample has not the time to be effected. Fig. 15 clearly shows us this result: both adiabatic and isothermal tension tests are represented versus tests with an external imposed temperature at both slow and high force rates.

5. Conclusion

In this paper, the numerical implementation of the asymmetric pseudoelastic behavior of SMA coupled with the heat equation has been done.

In a first part, a phenomenological model [1] has been implemented in COMSOL© in order to take into account this asymmetry between tension and compression and the

temperature effects. The thermodynamical coupling between the stress–strain and temperature is solved with the heat equation.

In the second part, for checking this implementation, many static tests have been performed: plate in tension, in bending loaded in its plane. These tests have clearly shown the influence of the type of solicitations (tension or compression) and the influence of the temperature on the pseudoelastic behavior of a SMA sample. At last, rate effects have been shown by loading a plate in tension with different force rates.

This study shows us the influence of the heat equation and the asymmetric aspect on the quality of the modelisation of the SMA. This taking into account appears essential for the modeling of SMA structures, particularly for complex dynamical SMA devices where the solicitations can be complex (tension and compression) and the temperature effects important (high frequency, thus adiabatic behavior). Typically, a slow rate loading test can be assimilated as a quasi static test. Thus, the SMA sample keep the temperature constant during this test. Hence, an external imposed temperature test with a high rate loading can be assimilated as an isothermal test. In the same way, an external imposed temperature test with a high rate loading can be assimilated as an adiabatic test: the heat transfer between the external field and the SMA sample has not the time to be effected. Fig. 15 clearly shows us this result: both adiabatic and isothermal tension tests are represented versus tests with an external imposed temperature at different force rates.

References

[1] B. Raniecki, C. Lexcellent, Eur. J. Mech. A/Solids 17 (2) (1998) 185–205.
[2] B. Raniecki, C. Lexcellent, K. Tanaka, Arch. Metall. 44 (3) (1992) 261–284.
[3] L.C. Brinson, Intell. Mater. Syst. Struct. 4 (1993) 229–242.
[4] S. Leclerq, C. Lexcellent, J. Mech. Phys. Solids 44 (1996) 953–980.
[5] C. Bouvet, S. Calloch, C. Lexcellent, J. Eng. Mater. Technol. 124 (2002) 112–124.
[6] M. Collet, E. Foltte, C. Lexcellent, Eur. J. Mech. A/Solids 20 (2001) 615–630.
[7] J. Rejzner, C. Lexcellent, B. Raniecki, Int. J. Mech. Sci. 44 (2002) (2001) 665–686.
[8] C. Bouvet. De l'uniaxial au multiaxial: comportement pseudoelastique des alliages a memoire de forme. Thesis, Universite de Fanche-Comte, 2001.
[9] K. Gall, H. Sehitoglu, H.J. Maier, K. Jacobus, Met. Mater. Trans. (1998) 765–773.
[10] C. Lexcellent, J. Rejzner, C. Bouvet, P. Robinet, S. Calloch, Comportement pseudolastique des alliages mmoire de forme sous sollicitations multiaxiales radiales, in: 39emeCongrs de Mtallurgie, Quebec, 1999, pp. 73–78.
[11] E. Patoor, M. El Amrani, A. Eberhadt, M. Berveiller, J. Phys. IV 2 (1995) 495–500.
[12] F. Auricchio, R.L. Taylor, J. Lubliner, Comput. Methods Appl. Mech Eng. 146 (1995) 281–312.
[13] D.P. Koistinen, R.E. Marbuger, Acta Metall. 7 (1959) 55–69.
[14] C. Lexcellent, J. Rejzner, Smart Mater. Struct. 9 (1998) 613–621.
[15] T. Jesse Lim, David L. McDowell, J. Eng. Mater. Technol. 121 (1999) 9–18.